

CORRELATIONS IN MULTIPARTICLE PRODUCTION  
(#46, 150, 166, 189, 190, 328, 329, 417, 756, 757, 758, 987)

Presented by R. Panvini  
Vanderbilt University  
Nashville, Tennessee

1. Introduction; Motivation for Correlation Studies

The single-particle inclusive reaction, i.e.,  $a + b \rightarrow c + \text{anything}$ , has been the processes most studied in attempts to uncover new dynamical features in multiparticle production processes involving hadronic interactions. It is clear, however, that to gain further insights it will be necessary to study correlations between particles produced two and more at a time.

Two salient features of particle production determined from the study of single particle spectra (originally from cosmic ray data) include:

- i) The transverse momentum ( $p_T$ ) of produced secondaries is strongly damped.
- ii) Colliding particles lose a relatively small fraction of their incident energy ( $\sim 50\%$ ) and emerge as "leading" secondary particles.

Recent inclusive data reveal a third feature:

iii) The spectra of secondaries plotted according to the prescriptions of Feynman or of Yang and coworkers exhibit a trend toward energy independence in the high energy limit.

Additional striking regularities gathered from years of study of accelerator data include:

iv) Resonances are copiously produced in all final-state multiplicities. The invariant mass distribution therefore reveals the most significant correlation between produced particles ever discovered.

v) Total and elastic cross sections exhibit asymptotic behavior at relatively low energies.

vi) Two-body and quasi-two-body reactions can be classified and their behavior at least qualitatively understood in terms of the quantum numbers exchanged in the  $t$ -channel. Inelastic processes that behave like elastic processes are those where the vacuum quantum numbers are exchanged.

The purpose of studying correlations is to attempt to find additional regularities which stand out sufficiently well that they can be added to the above list of dynamical features, which in turn must be incorporated in any model or theory of hadronic processes. Any correlations which are a consequence of already well-known features must be understood. However, they should not be confused with new features of data.

2. Two-Particle Correlations; Correlation Function

The procedure adopted by many experimenters for studying two-particle correlations is by means of a correlation function. A more complete description of these procedures is given by LeBellac.<sup>1</sup> Here we reiterate some essential points.

The standard correlation function, based on the liquid/gas analogy of Feynman and Wilson,<sup>2</sup> is

$$C_2(y_1, y_2) = \frac{1}{\sigma_T} \frac{d^2\sigma}{dy_1 dy_2} - \frac{1}{\sigma_T^2} \left( \frac{d\sigma}{dy_1} \right) \left( \frac{d\sigma}{dy_2} \right). \quad (1)$$

The variables  $y_{1,2}$  are usually either the rapidities [ $y \equiv 1/2 \ln (E + p_{\parallel})/(E - p_{\parallel})$ ] or the Feynman scaling variables ( $x \equiv p_{\parallel}^*/p_{\parallel, \text{max}}^*$ ), and  $\sigma_T$  is the total inelastic cross section.

The first term in expression (1) is analogous to the probability of finding gas molecules simultaneously at locations  $r_1$  and  $r_2$  in a one-dimensional gas; the second term is analogous to the probability of finding a single molecule at coordinate  $r_1$  multiplied by the probability of finding another at coordinate  $r_2$ . Therefore if  $C_2(y_1, y_2)$  is zero for all values of  $y_1$  and  $y_2$  this procedure tells us that the two particles are uncorrelated in the  $y_1$  and  $y_2$  variables. Another way of defining the correlation function is to compute

$$\tilde{C}_2(y_1, y_2) = \frac{\frac{1}{\sigma_T} \frac{d^2\sigma}{dy_1 dy_2}}{\frac{1}{\sigma_T^2} \left( \frac{d\sigma}{dy_1} \right) \left( \frac{d\sigma}{dy_2} \right)}. \quad (2)$$

With this definition,  $\tilde{C}_2 = 1$  for all  $y_1$  and  $y_2$  means that there are no correlations.

Some essential differences between molecules in a gas and produced hadrons must be understood:

a) Kinematics. Energy and momentum conservation prevents both particles simultaneously having values of  $y$  near the maximum value allowed for one particle at a time.

b) Multiplicities. Unlike the typical numbers of molecules in a gas the average number of produced hadrons is small and multiplicities vary over a wide range. It is essential to understand how different multiplicities contribute when interpreting a correlation function.

c) Normalization. Because of items (a) and (b), the standard definition (1) of the correlation function may not be the most sensible one. The use of  $\sigma_T$  and  $\sigma_T^2$  as normalizing factors in the two terms is not totally obvious. The proper normalizing factors depend on particle types, multiplicities considered, and kinematic, and kinematic restrictions.

### 3. Two Particle Correlation Data

To understand better the significance of the correlation function, we will examine in more detail the properties of the single particle distribution  $d\sigma/dy$  and the double differential cross section  $d^2\sigma/dy_1 dy_2$ . For example, the single particle spectrum is well fitted by a gaussian for four through twelve prong events from the reaction  $pp + \pi^- + X$  at 28.5 GeV/c.<sup>3</sup> The expression used is

$$\left. \frac{d}{dy} \right|_n = \frac{n\sigma_n}{S_n \sqrt{2\pi}} e^{-\left( \frac{y^2}{2S_n^2} \right)}$$

when  $n$  is the number of negative pions. In Fig. 1 it is shown how  $S_n$ , the gaussian width, decreases as  $n$  increases. Preliminary data of the Pisa-Stony Brook collaboration<sup>4</sup> from the ISR show the same trend of a narrowing spectrum with increasing multiplicity (Fig. 2).

The double-differential cross section for  $\pi^-\pi^-$  production in  $pp + \pi^-\pi^- + X$  at 28.5 GeV is studied by fitting

$$\frac{d^2\sigma}{dy_1 dy_2} = \frac{A}{S\sqrt{2}} e^{-\frac{(y_2 - \bar{y}_2)^2}{2S^2}}$$

for each of various intervals of  $y_1$ . The mean value  $\bar{y}_2$  and the gaussian width  $S$  is plotted as a function of  $y_1$  as shown in Fig. 3. Both  $\bar{y}_2$  and  $S$  are independent of  $y_1$  except when  $y_1$  is large and kinematic constraints become important. Plots of  $d^2\sigma/dy_1 dy_2$  for various intervals in  $y_1$  from the 21 GeV/c data,  $p\bar{p} + \pi^-\pi^- + X$ , of Berger et al.<sup>5</sup> are shown in Fig. 4 revealing again that the distribution in  $y_1$  is essentially independent of  $y_2$ . Superimposed on the distributions are curves that represent the Nova model fits to the data. The significance of the Nova model fit is that the input to the model is only what is already known from single particle distributions.

Braun et al.<sup>6</sup> investigated the correlation function for all possible pion pairs in the reaction  $p\bar{p} + 3\pi^+ 3\pi^- \pi^0$  at 5.7 GeV/c. They point out (see Fig. 5) that kinematic constraints produce rounded corners in the  $y_1$ - $y_2$  or  $x_1$ - $x_2$  planes. If  $C_2(y_1, y_2)$  is computed where only the single particle distribution is nonzero, i.e., both  $y_1$  and  $y_2$  are large, then  $C_2$  will automatically be negative. To avoid this kinematic effect  $C_2$  should be computed for  $y_1, y_2$  or  $x_1, x_2$  values sufficiently far from the boundaries.

The influence of separate multiplicities on  $C_2$  is strikingly demonstrated by Diamond and Erwin.<sup>7</sup> They examine  $\pi^+\pi^+$  and  $\pi^+\pi^-$  pairs in the reaction  $\pi^-p + \pi\pi + X$  at 24.8 GeV/c.  $C_2$  is plotted against the  $y$ -value of one of the two pions while the  $y$ -value of the second pion is held fixed. The data are displayed for all multiplicities, for all but the two prongs, and finally, for all but both the two and the four prongs. These results are shown in Fig. 6. Strong variation is seen in the overall  $C_2$  distributions but the variations decrease considerably when the two prongs are removed, and even more so when the four prongs are removed. This is understood by the fact that the low multiplicities contain the quasi-two-body channels where particles are clearly separated into forward and backward components.  $C_2(\pi^-\pi^-)$  will necessarily be negative for two prong events since only the second term contributes.

A modified correlation function  $C_2'(\pi^-\pi^-)$  is examined for each multiplicity separately in  $p\bar{p} + \pi^-\pi^- + X$  at 28.5 GeV/c by Hanlon et al.<sup>3</sup> In this instance the lowest multiplicity is six prongs and one finds (since the variation of  $y_2$  is largely independent of  $y_1$  as shown in Fig. 2) that  $C_2'(\pi^-\pi^-)$  is likewise zero or close to zero for all  $y_1$  and  $y_2$ . The variations in  $C_2'$  represent no more than 10% ripples above a uniform background.

The Aachen-Berlin-CERN-London-Vienna collaboration<sup>8</sup> examine the inclusive process  $K^-p + \bar{K}^0 p + X$  at 10 GeV/c; they interpret the final state  $\bar{K}^0$  and  $p$  as the leading particles in this reaction. A Monte Carlo simulation of this reaction is made by adding the various multiplicities with appropriate weights; the matrix element applied is

$$M^2 = \exp\left(-\sum_{\text{pions}} p_{\parallel}^2\right) \cdot [\exp(1.7t_{pp}) \cdot \exp(0.7t_{kk})],$$

where the first term takes into account the damping in transverse momentum of produced pions and the second term builds in the leading-particle effect. It is shown

that  $\bar{K}$ -p correlations computed in terms of a correlation function  $C_2(x_k, x_p)$  can be reproduced very well by this model which uses as input only what is already known from single-particle distributions. The comparison between data and model is shown in Fig. 7 where the magnitudes and signs of  $C_2[x(k), x(p)]$  are plotted as a function of  $x(k)$  and  $x(p)$ .

The Pisa-Stony Brook collaboration<sup>4</sup> have preliminary results on  $p + p + S(1) + S(2) + X$  from the ISR; they measure the cm angles of particles  $S(1)$  and  $S(2)$  and compute  $\eta = -\log \tan(\theta/2)$  which is the same as rapidity,  $y$ , when  $p_1^2 \gg m^2$ . In Fig. 8 is shown a plot of the function

$$\tau_2(\eta_1, \eta_2) = N_I \frac{N(\eta_1, \eta_2)}{N(\eta_1)N(\eta_2)}$$

as a function of the difference  $\eta_1 - \eta_2$  for various intervals in  $\eta_1$ .  $N_I$  is the total number of inelastic events,  $N(\eta_1)$  is the number of events with a charged particle at  $\eta_1$ , and  $N(\eta_1, \eta_2)$  is the number of events with charged particles at both  $\eta_1$  and  $\eta_2$ . This quantity should be constant and equal to unity if there are no correlations; instead they see a strong tendency for particles to emerge preferentially with small differences in  $\eta_1 - \eta_2$  almost independent of  $\eta_1$ .

A CERN group<sup>9</sup> studied  $p + p + \gamma_1 + \gamma_2 + X$  at the ISR and they plot

$$\frac{d^2\sigma}{dy_1 dy_2} / \frac{1}{\sigma_T} \left( \frac{d\sigma}{dy_1} \right) \left( \frac{d\sigma}{dy_2} \right)$$

versus  $|y_2 - y_1|$  for different  $y_1$  values (Fig. 9). Their results show a flat distribution in contradiction with the Pisa-Stony Brook data. At present, no more can be said except that both sets of data are preliminary.

#### 4. Correlations Involving More than Two Particles at a Time

From an exposure of the Argonne 30-inch hydrogen bubble chamber at NAL to 205 GeV protons,<sup>10</sup> an event-by-event display was made of 31 individual events. As shown in Fig. 10, the quantity  $\log \tan(\theta_{lab}/2)$  is plotted for each charged track. Nothing striking appears from a visual examination of these events. However, a procedure that has been applied to 28 GeV pp and pd data by Panvini et al.<sup>11</sup> may be useful for further analysis of the 200 GeV events. The reactions studied were  $pd + (p_s)pp\pi^-$ ,  $pp + pp\pi^+\pi^-$ ,  $pd + (p_s)pp\pi^-\pi^-\pi^+$ , and  $pp + pp\pi^+\pi^-\pi^+\pi^-$  (related studies have been made by Shapira et al.<sup>12</sup> for  $pp + pp\pi^+\pi^-$  at several energies). For every event the rapidity,  $y$ , is computed for every track as in the event-by-event plot shown in Fig. 10. It is noted that

$$y = \frac{1}{2} \ln \frac{E + p_{||}}{E - p_{||}} = \frac{1}{2} \ln \frac{1 + \beta_{||}}{1 - \beta_{||}},$$

i.e., that  $y$  depends only on the longitudinal velocity of particles. Hence, if particle production results from the decay of massive clusters, one might expect that groups of particles would be found with values of rapidity close to each other. In analyzing the 28 GeV data, cluster production is operationally defined by arranging the particles into two groups that lie on either side of the largest gap in rapidity space between adjacent particles. This procedure reveals, as expected, the dominance of diffractive production in the one- and two-pion channels but it is also seen that single cluster production (meaning that there is a proton opposite everything else) dominates in three- and four-pion production as well. This may

just be a reflection of the leading particle effect. The same procedure applied to 200 GeV data might be expected to work better since there is more room in the phase space for particle production of not too high multiplicities.

Finally, we note a very interesting preliminary result of the Stony Brook-Pisa collaboration at the ISR.<sup>4</sup> They compare multiplicities and angular distributions in the left hemisphere with those in the right hemisphere. Indications are that both multiplicities and angular distributions in one hemisphere are independent of what is occurring in the opposite hemisphere. Furthermore, looking downstream of one incident proton at a fixed energy, the multiplicity and angular distributions are independent of the energy of the second incident proton.

#### 5. Summary and Conclusions

Studies of correlations among two and more particles at a time for energies below  $\sim 30$  GeV have not yet revealed any striking new features; the gross distribution of particles is at least qualitatively understood in terms of things we already know about particle production. The low multiplicity events show correlations that are to be expected from the quasi-two-body channels. The higher multiplicity events are qualitatively described by assuming that the only constraints besides energy and momentum conservation are the characteristics well-known from single particle spectra; the transverse momenta are sharply damped and there are leading particles which preserve the identity of the incident particles.

Strong correlation effects are more likely to be seen at ISR/NAL energies. The preliminary results of the Pisa-Stony Brook<sup>4</sup> group already include what appear to be significant correlations. A theoretical prediction by J. Ranft and G. Ranft<sup>13</sup> has been made to illustrate the striking difference that would be expected in the two particle correlation function at 1500 GeV between multiperipheral-type models and diffractive-type models. The predictions shown in Fig.11 are very obviously different for the two contrasting cases. Plotted are contours representing the magnitude of the correlation function  $\hat{C}_2(y_1, y_2)$  over the range of values of  $y_1$  and  $y_2$ .

#### References

<sup>1</sup>M. LeBallac, "Correlations in Inclusive Reactions," invited talk in parallel sessions (see High-Energy Collisions IV, summary by A. H. Mueller, this volume).

<sup>2</sup>R. P. Feynman, High-Energy Collisions, Proc. of Third International Conference, Stony Brook (1969); K. Wilson, Cornell University preprint CLNS-131 (1970).

<sup>3</sup>J. Hanlon et al., Study of  $\pi^-\pi^-$  Correlations in the Reaction  $pp \rightarrow \pi^-\pi^- + \text{Anything}$  at 28.5 GeV, #190.

<sup>4</sup>Private communication by G. Belletini for the Pisa-Stony Brook collaboration.

<sup>5</sup>E. L. Berger et al., Two Particle Correlations in Inclusive  $pp$  Interactions Between 13 and 28 GeV/c, #150. Figure 4 is actually a private communication from E. L. Berger, Ma, Oh, and Smith.

<sup>6</sup>H. Braun et al., Two Particle Correlation in the  $\bar{p}p \rightarrow 3\pi^+ 3\pi^- \pi^0$  Reaction at 5.7 GeV/c, #46.

<sup>7</sup>R. N. Diamond and A. R. Erwin, Pion-Pion Correlations in 25 GeV/c  $\pi^- p$  Collisions, #417.

<sup>8</sup>J. V. Beaupre et al., Aachen-Berlin-CERN-London-Vienna collaboration, #166.

<sup>9</sup>G. Flügge et al., Single and Double Photon Production in  $pp$  Collisions at the ISR, CERN, #'s 757 and 758.

<sup>10</sup>G. Charlton et al., Argonne-NAL-Iowa State-Michigan State-Maryland collaboration, #987.

<sup>11</sup>W. Burdett et al., Evidence for Two Cluster Formation in One-, Two-, Three-, and Four-Pion Production in 28 GeV/c pp and pd Collisions, #189.

<sup>12</sup>A. Shapira, Rapidity Analysis of Exclusive Hadron Reactions, #328; A. Shapira et al al., World  $pp\pi^+\pi^-$  Collaboration, Energy Dependence of reaction Characteristics and Cluster Formation in the Reaction  $pp \rightarrow pp\pi^+\pi^-$  at  $P_{lab} = 5$  Through 22 GeV/c, #329.

<sup>13</sup>J. Ranft, private communication; also J. Ranft and G. Ranft, #756.

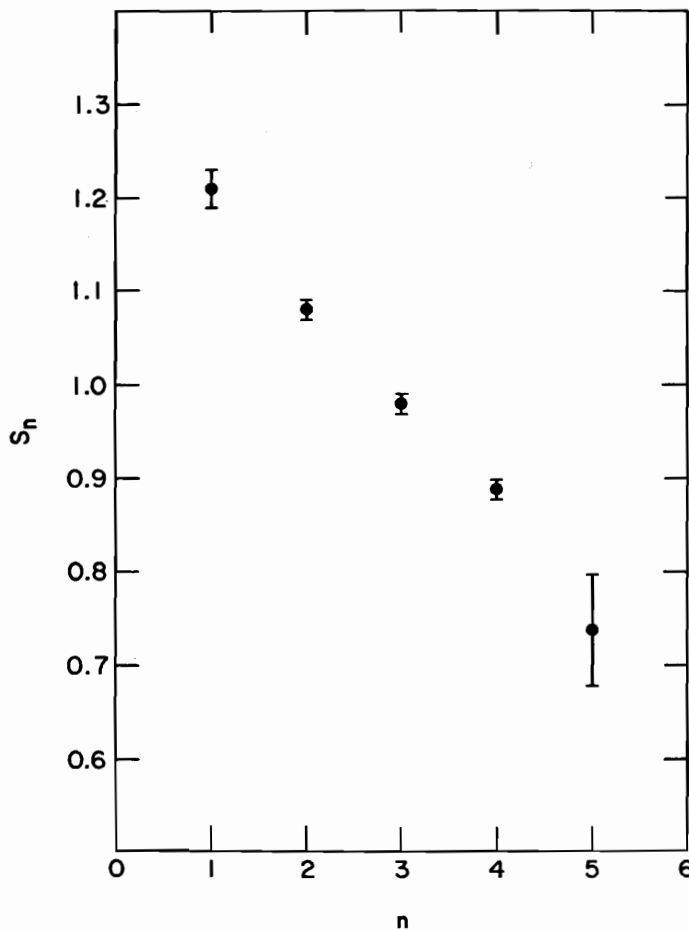


Fig. 1. Gaussian width  $S_n$  of the distribution

$$\left. \frac{d\sigma}{dy} \right|_n = \frac{n\sigma_n}{S_n \sqrt{2\pi}} e^{-\left(\frac{y^2}{2S_n^2}\right)}$$

versus  $n$  for the reaction  $pp + \pi^- + X$  at  $28.5 \text{ GeV}/c$  (Hanlon et al.<sup>3</sup>).

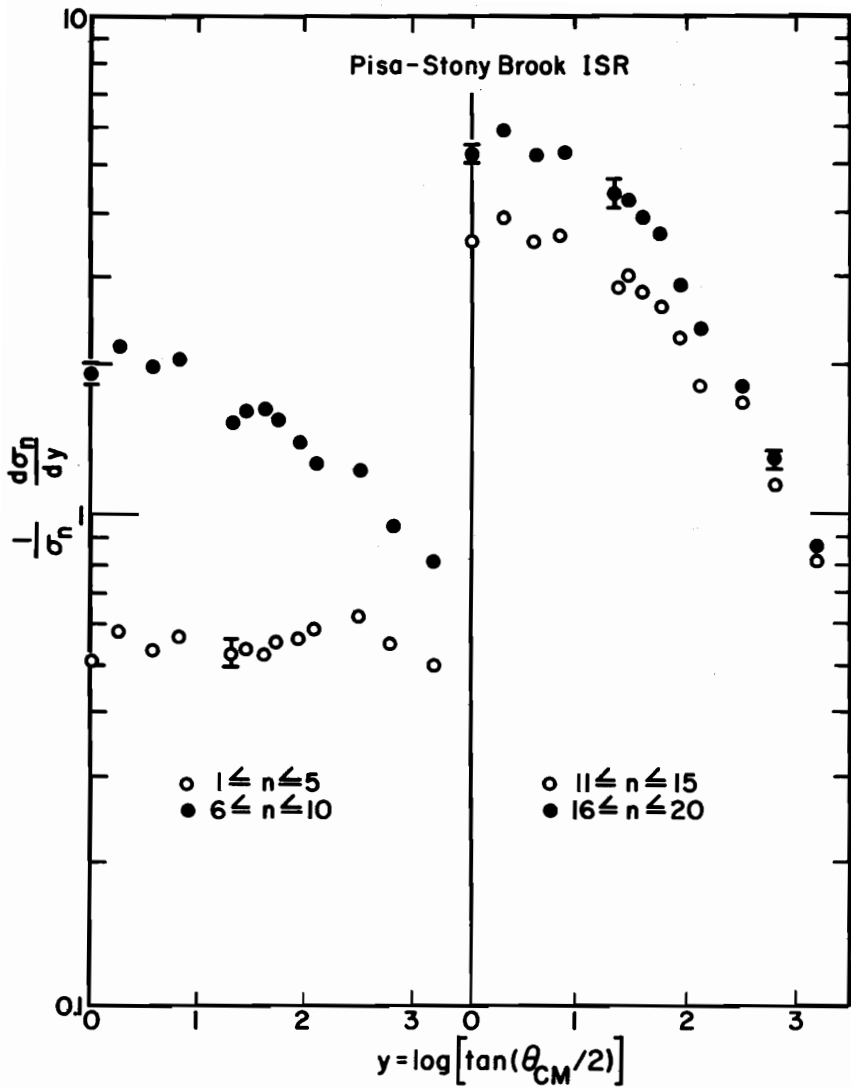


Fig. 2. Plot of  $(1/\sigma) (d\sigma/dy)$  versus  $y$  for various multiplicities from ISR data of Pisa-Stony Brook collaboration.<sup>4</sup>

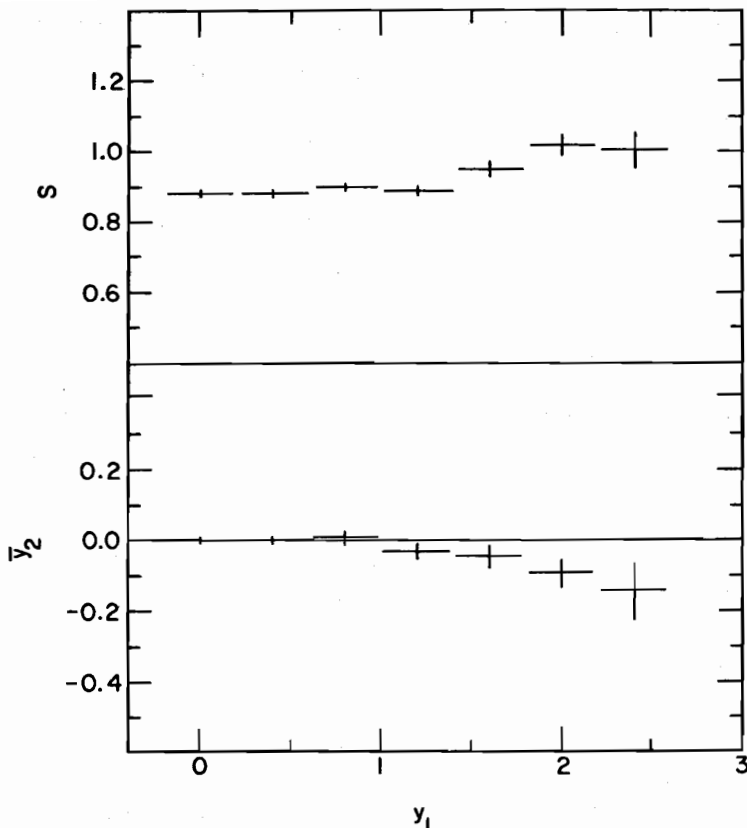


Fig. 3. Plot of  $\bar{y}_2$  and  $S$  versus  $y_1$  for the distribution

$$\frac{d\sigma}{dy_1 dy_2} = \frac{A}{S\sqrt{2\pi}} e^{-\frac{(y_2 - \bar{y}_2)^2}{2S^2}}$$

from  $pp + \pi^-\pi^+ + X$  at 28.5 GeV/c (Hanlon et al.<sup>3</sup>).

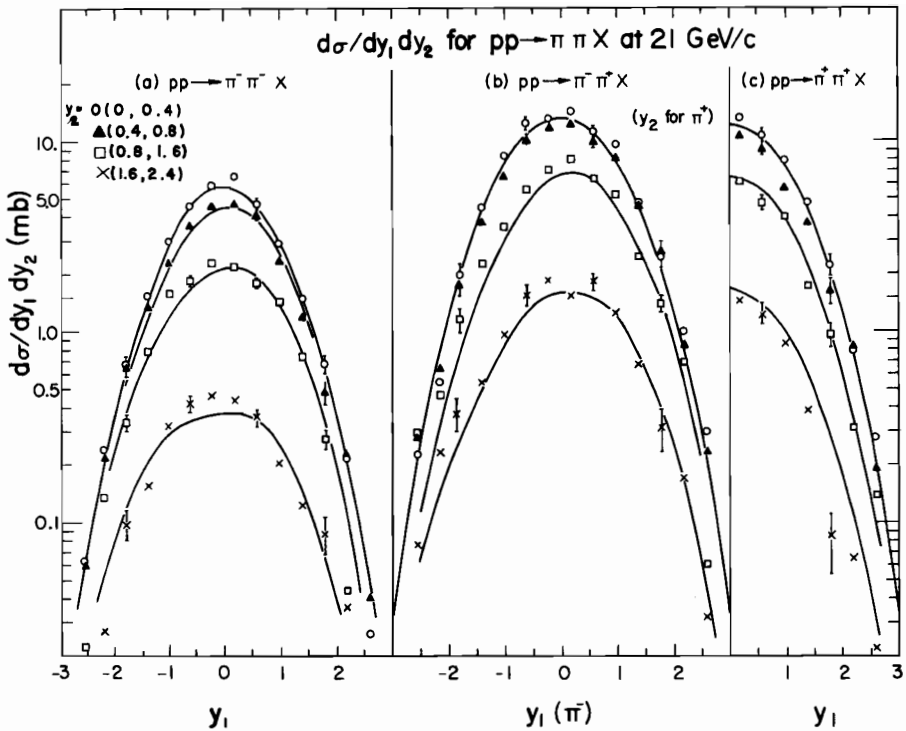


Fig. 4.  $d\sigma/dy_1 dy_2$  versus  $y_1$  for various cuts on  $y_2$  in the reaction  $pp \rightarrow \pi\pi + X$  at 21 GeV/c (Berger et al.<sup>5</sup>).  
 Curves are Nova model fits.

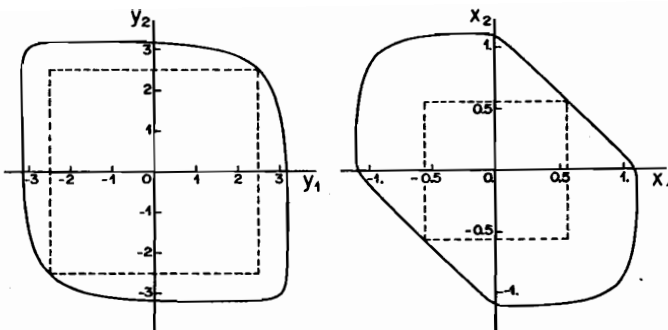


Fig. 5. The kinematic boundaries (heavy lines) in the  $x_1, x_2$  and  $y_1, y_2$  scatter plots obtained for a pion pair in the  $\bar{p}p + 7\pi$  reaction at 5.7 GeV/c. The biggest squares contained within these boundaries and having their sides parallel to the coordinate axes (dashed lines) contain pion pairs for which the kinematical limits of the two terms entering into the correlation function are identical (Braun et al.<sup>6</sup>).

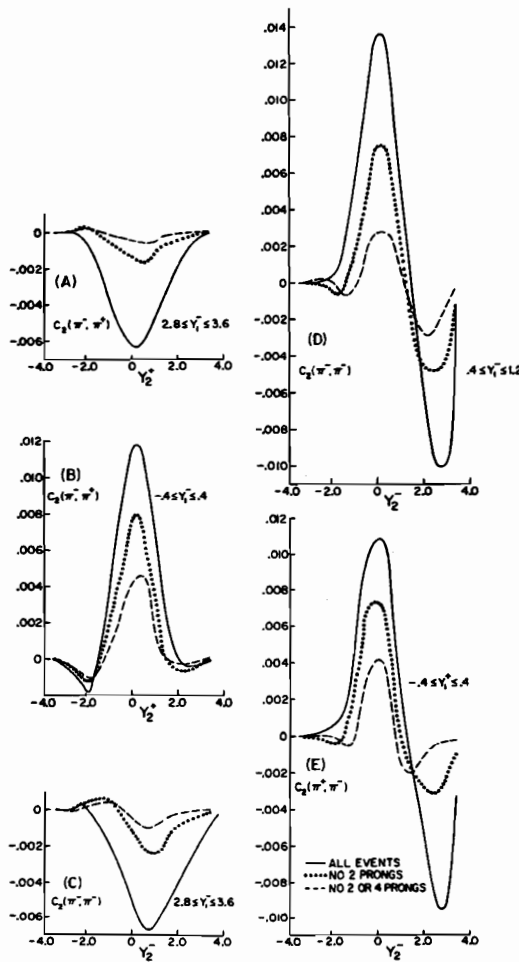


Fig. 6. Correlation functions  $C_2(\pi^-, \pi^+)$ ,  $C_2(\pi^-, \pi^-)$ , and  $C_2(\pi^+, \pi^-)$  plotted as a function of  $y_2$  for various intervals of  $y_1$  from the 24.8 GeV/c  $\pi^- p$  data of Diamond and Erwin.<sup>7</sup>

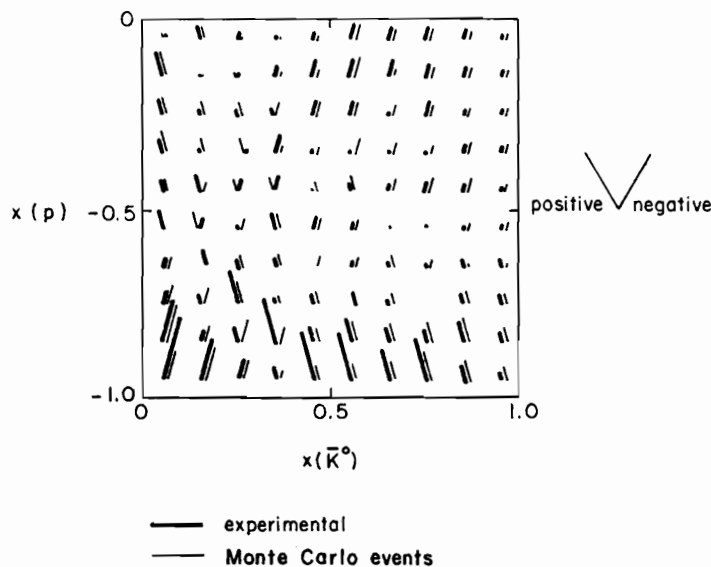


Fig. 7. Comparison of the values of the experimental correlation function in each  $\Delta x_p \cdot \Delta x_{\bar{K}}$  bin with the corresponding values of the correlation function generated by Monte Carlo method for the reaction  $K^- p \rightarrow \bar{K}^0 p + X$  at 10 GeV/c (Beaupre et al.<sup>8</sup>).

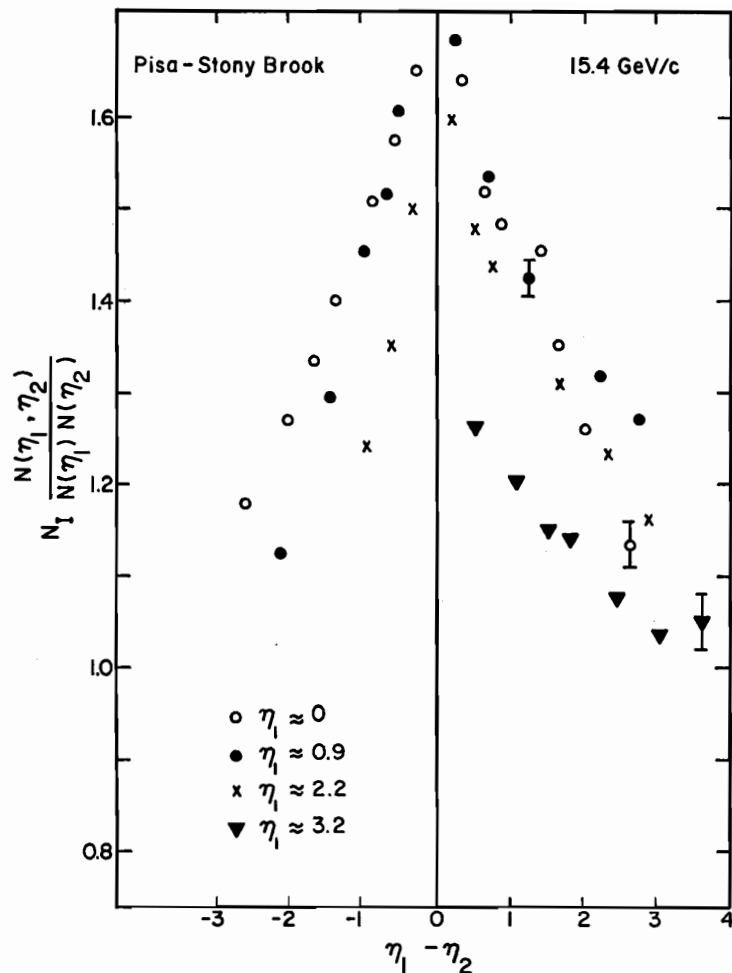


Fig. 8. Plot of the quantity

$$\frac{N(\eta_1, \eta_2)}{N_1 \frac{N(\eta_1, \eta_2)}{N(\eta_1)N(\eta_2)}}$$

versus  $\eta_1 - \eta_2$  for various  $\eta_1$  (Pisa-Stony Brook collaboration<sup>4</sup>) from ISR data on  $pp \rightarrow$  (Particle 1) + (particle 2) + anything at c.m.s. energy of 30.8 GeV.

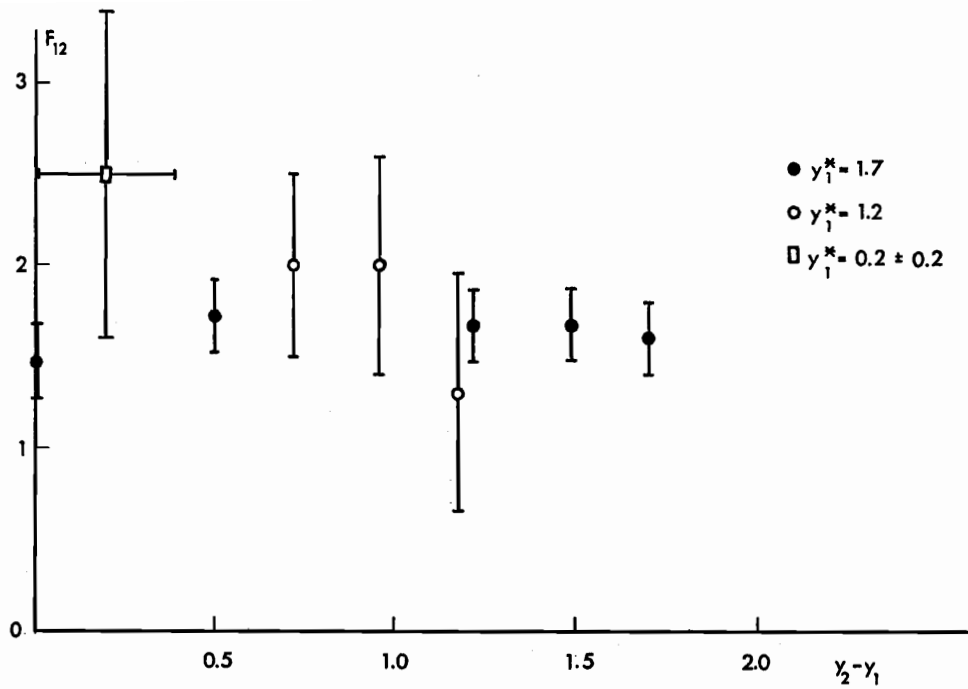


Fig. 9. Plot of the correlation function

$$F_{12} = \frac{\frac{d^2\sigma}{dy_1 dy_2}}{\frac{1}{\sigma_T} \left( \frac{d\sigma}{dy_1} \right) \left( \frac{d\sigma}{dy_2} \right)}$$

versus  $y_2 - y_1$  for fixed values of  $y_1$  (Flügge et al.<sup>9</sup>) from ISR data on  $pp + y_1 + y_2 + \text{anything}$ .

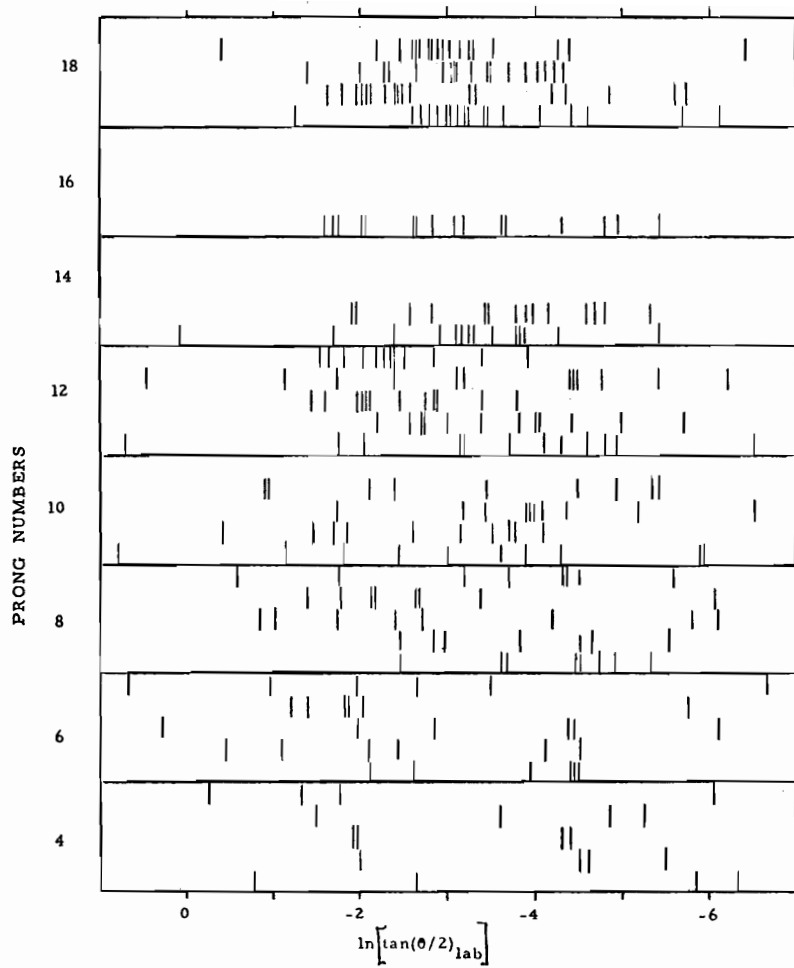


Fig. 10. The individual values of  $\ln [\tan(\theta/2)_{\text{lab}}]$  for 31 events from Charlton et al.<sup>10</sup> 205 GeV pp bubble chamber experiment.

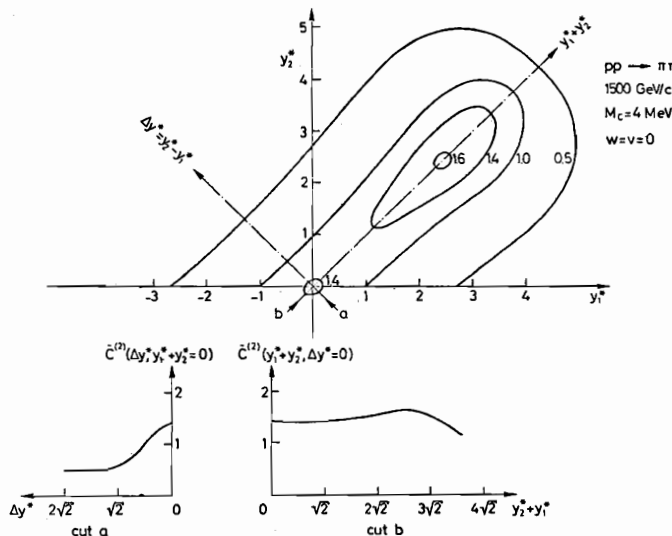


Fig. 11(a). Multiperipheral model prediction of Ranft et al.<sup>13</sup> for the magnitude of the two particle correlation function  $\bar{C}_2(y_1^*, y_2^*)$  in terms of  $y_1^*$  and  $y_2^*$  for  $pp \rightarrow \pi\pi + x$  at 1500 GeV.

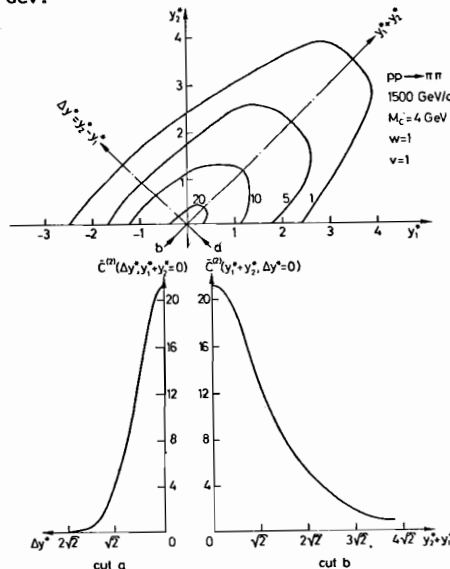


Fig. 11(b). The same as (a) but for the diffractive model.